

## Article

# Effect of Agitation Methods on Characteristics of Iron Ferrite Nanoparticles Synthesized by Co-Precipitation Process

Hamid Reza Dehghanpour<sup>1,\*</sup>, Parviz Parvin<sup>2</sup>, Aryan Younesi<sup>3</sup>, Monireh Gilaki<sup>4</sup>

<sup>1</sup> Department of Physics, Tafresh University, Tafresh 3951879611, Iran

<sup>2</sup> Physics Department, Amirkabir University of Technology, P.O. Box 15875-4413, Tehran, Iran, [Parvin@aut.ac.ir](mailto:Parvin@aut.ac.ir)

<sup>3</sup> Department of Chemical Engineering, Tafresh University, Tafresh 3951879611, Iran, [yunesi@tafreshu.ac.ir](mailto:yunesi@tafreshu.ac.ir)

<sup>4</sup> Department of Physics, Tafresh University, Tafresh 3951879611, Iran, [mon.gilaki@gmail.com](mailto:mon.gilaki@gmail.com)

\* Correspondence: [h.dehghanpour@aut.ac.ir](mailto:h.dehghanpour@aut.ac.ir)

Received: Aug 10, 2022; Accepted: Sep 10, 2022; Published: Sep 30, 2022

**Abstract:** To assess the result of the stirring process on the Fe<sub>3</sub>O<sub>4</sub> nanoparticles' properties, two types of stirrings (mechanical and magnetic) were compared. Fe<sub>3</sub>O<sub>4</sub> nanoparticles were generated by chemical precipitation. Oleic acid covered the nanoparticles as a surfactant performer. X-ray diffraction (XRD) was used to investigate the fine grains sample, and scanning electron microscope (SEM) images were used for observing the nanoparticles' geometry. The vibrating sample magnetometer (VSM) was also used to examine the magnetic characteristic of the nanoparticles. Chemical bonds were determined by using Fourier transform infrared spectroscopy (FTIR). As a result, the hysteresis loop characterized the magnetic nanoparticles. Magnetite nanoparticles are regarded as a soft magnetic material due to their low coercivity. XRD diagrams show the presence of powerful peaks in the orientations of crystal surfaces of the spinel form of the nanoparticles. The result showed that nanoparticles were nearly spherical. The average dimensions of the nanoparticles were estimated by Scherrer approximation. The mean particle dimensions were 11 nm (chemical mixer) and 13 nm (magnet mixer). SEM images verified the spherical shape of the nanoparticles, and FTIR confirmed the constitution of Fe-O bonds and validated the spinel ferrites configuration.

**Keywords:** Fe<sub>3</sub>O<sub>4</sub> Ferrite, Nanoparticle, precipitation, Spinel

## 1. Introduction

Tiny magnetic particles are noticeable in many fields [1–5]. High crystalline nanoparticles are used in a wide range of technical fields. Ferrite spinel nanoparticles exhibit superparamagnetic properties due to the distinctive electrical and magnetic characteristics of spinel ferrites. Thus, they are commercially valuable. There are many reports about the synthesis processes of ferrite nanoparticles by different methods: sol-gel [6–8], co-precipitation [9–11], hydrothermal [12–14], chemical mechanics [15], refluxing [15,16], thermal decomposition [17], solvothermal method [18], ultrasonic bath [19], laser ablation [20, 21], microwave [22], precursor [23] and combustion [24–28]. Due to the remarkable properties of iron oxide magnetic nanoparticles such as superparamagnetism, high coercivity, low Currier temperature, high magnetic sensitivity, non-toxicity, biocompatibility, and low production cost, much research attention has been in this field [29–31]. Among all the properties, the magnetic property is significantly dependent on the size of the nanoparticles. Ferromagnetic materials contain the areas containing the groups of spins that have similar orientations and are separated by the walls of the domains. By reducing the particle size, the walls of these domains do exist in terms of energy with only one domain. Therefore, superparamagnetic phenomena occur [32] in which there is a great deal of interest in research and applications.

There are various methods for the preparation of Fe<sub>3</sub>O<sub>4</sub> nanoparticles, including arc discharge, microemulsion, mechanical milling, laser ablation, sol-gel and high-temperature decomposition of organic and sonochemical precursors, and so on. The co-precipitation method can be considered a desirable alternative to conventional powder production techniques with proper control of Fe<sub>3</sub>O<sub>4</sub> nanoparticles owing to low production cost and low-temperature process. The chemical co-precipitation method produces high-purity metal oxides. On the other hand, if in this method, the production conditions such as solution pH, process temperature, the concentration of solutes and surfactants and stirring speed are well controlled, nanoparticles with the desired shape and size are synthesized. Here, Fe<sub>3</sub>O<sub>4</sub> magnetic nanoparticles are synthesized using the co-precipitation method. Magnetic and geometric properties of the nanoparticles are investigated via VSM, SEM, and XRD. The FTIR is utilized to confirm the constitution of Fe-O

bonds and validated the spinel ferrites configuration in the octahedral and tetrahedral sites related to the spinel configuration. This is a complement to the previous results [33,34].

## 2. Materials and Methods

The reagents used for the synthesis included ferric chloride ( $\text{FeCl}_3 \cdot 6\text{H}_2\text{O}$ ) and ferrous chloride ( $\text{FeCl}_2 \cdot 4\text{H}_2\text{O}$ ) salts in the molar ratio of 1:2,  $\text{Na}(\text{OH})$ ,  $\text{HCl}$ , Oleic acid, and ethanol. Water was also used as a solvent. All materials were used without additional purification. The reaction in the process was as follows.



Two mixtures were produced via mixing of 1ml (2 moles) of ( $\text{FeCl}_2 \cdot 4\text{H}_2\text{O}$ ) and 4ml (1 mole) of ( $\text{FeCl}_3 \cdot 6\text{H}_2\text{O}$ ) as long as 2000 rpm stirring for separation mechanically and magnetically for 3 min. Then, 25 ml of 1 mole  $\text{Na}(\text{OH})$  solution was added in drops to the mixtures. Immediately, the color changed to dark black in the solution (magnetite feature) for both samples. For removing the anionic electric charge on the nanoparticles outside, 0.5 ml of 2 moles of  $\text{HCl}$  was added to the mixture. The reactants were stirred with a magnetic stirrer during precipitation. Then, 5 ml of surfactant and coating (oleic acid) was added to the solution. At the reaction temperature of  $80^\circ\text{C}$ , the precipitation liquids were stirred for 1 h till the temperature dropped to room temperature. The precipitates were washed with deionized distilled water to remove impurities in the final products and then with ethanol to remove excess surfactants from the solutions. To separate the supernatant liquids (ethanol plus water), the mixtures were centrifuged. The supernatants were then drained. The centrifugation was continued until a thick black precipitate remained. The remaining sediments were dried for 24 h and ground into fine powder to make two samples for analysis using XRD, FTIR, SEM, and VSM.

## 3. Results and Discussion

Figure 1(a) depicts the XRD diagram of the produced nanoparticles using magnetic stirring. Figure 1(b) shows the XRD diagram of the nanoparticles generated by mechanical stirring. Characteristic peaks for  $\text{Fe}_3\text{O}_4$  labeled by their Miller indices ((220), (311), (400), (422), (511) and (440)) were distinguished in both samples. These peaks indicate that generated nanoparticles were nearly pure spinel forms of  $\text{Fe}_3\text{O}_4$ . The particle size is estimated from the broadening of diffraction peaks. The mean nanoparticle size is evaluated by the Debye-Scherrer equation,  $d = k\lambda/\beta\cos\theta$ . Here,  $d$  is the mean dimension of the crystallite, and  $k$  represents the constant Debay-Scherer coefficient (0.89). At the X-ray wavelength of  $1.54056 \text{ cm}^{-1}$ , the line broadening (in radians) is denoted by  $\beta$  which is obtained by measuring the full width at half of the maximum peaks and  $\theta$  specifying the Bragg angle. Using the Debye-Scherrer equation, the crystalline sizes were estimated to be  $\sim 11$  and  $\sim 13$  nm for mechanical and magnetic stirrer samples, respectively. The lattice parameter, obtained by the XRD data, is found to be in the range of  $8.3582$  to  $8.3651 \text{ \AA}$ .

The magnetic properties of the nanoparticles such as a saturation magnetization ( $M_s$ ) and a coercive field ( $H_c$ ) at room temperature are evaluated using VSM with a magnetic field in the range of  $-1000$  to  $1000$  Oe, (Fig. 2). The behavior of nanoparticles is generally determined by their magnetic properties. By applying a magnetic field  $H$ , the magnetic moment ( $\mu$ ) of the particle tries to be parallel to the direction of the magnetic field. The saturation magnetization of nanoparticles produced in mechanical stirring was  $8.136 \text{ emug}^{-1}$ , and for that of the magnetically stirred sample was  $13.85 \text{ emug}^{-1}$ . The Coercivity of the nanoparticles was small, indicating that the magnetic nanoparticles were superparamagnetic.

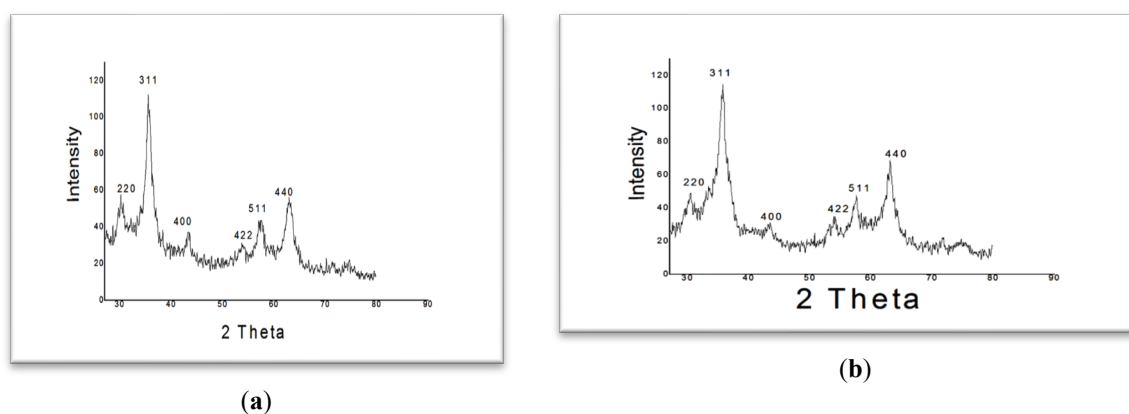
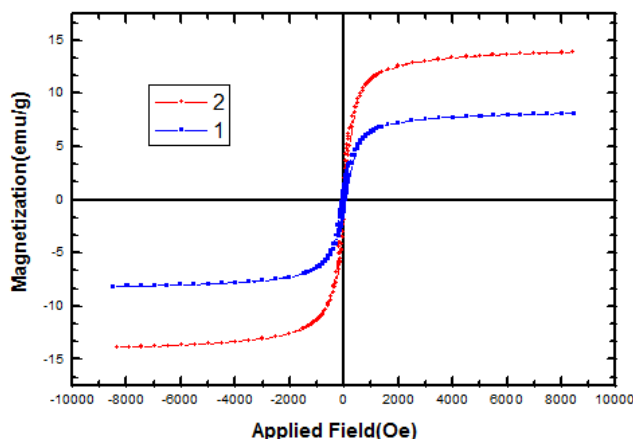


Fig. 1. X-ray pattern for  $\text{Fe}_3\text{O}_4$  nanoparticles produced by (a) magnetic and (b) mechanical stirring [33].



**Fig. 2.** VSM diagrams of the magnetic nanoparticles synthesized by mechanical stirring (curve 1) and magnet stirring (curve 2).

The saturation magnetization of the nanoparticles depends on their size. The larger nanoparticle's size results in the larger saturation magnetization. The saturation magnetization of a single domain depends on the number of magnetic moments within it. The particle with a larger size has more magnetic moments and a larger saturation magnetization. This behavior is related to a reduced particle size which leads to increasing disordering of the magnetic moment directions on the external surfaces of the particles. It results in a reduction in the particle's saturation magnetization. Due to the growth in the order of the system's magnetic moment's directions, the saturation magnetization reduces.

Figures 3 (a) and (b) depict the FTIR spectra of the Fe<sub>3</sub>O<sub>4</sub> nanoparticles synthesis by different stirring. In Figs. 3(a) and (b), the absorption band is observed at 553 and 557 cm<sup>-1</sup>. Figure 3 (b) shows the vibration of the Fe-O functional group corresponding to the tetrahedral sites of the ferrite spinel structure. The two peaks around 3407 cm<sup>-1</sup> in Fig. 3 (a) and 3406 cm<sup>-1</sup> in Fig. 3(b) are associated with the hydroxyl (OH<sup>-</sup>) group. Corresponding absorption bands for the C-H group are distinguishable at 2852 and 2853 cm<sup>-1</sup> (Figs. 3 (a) and (b)), respectively. The peaks at 1445 cm<sup>-1</sup> in Fig. 3(a) and 1441 cm<sup>-1</sup> in Fig. 3 (b) belong to the C-O group.

Figures 4 (a) and (b) show the SEM graphs of the samples. The shape of the nanoparticles is nearly spherical, which shows that there is an aggregation between the nanoparticles. The aggregation arises from the low concentration of surfactants in the colloidal solution or due to a drying process. Utilizing the oleic acid surfactant for sample coating plays an important role in the heat drying of the samples for aggregation.

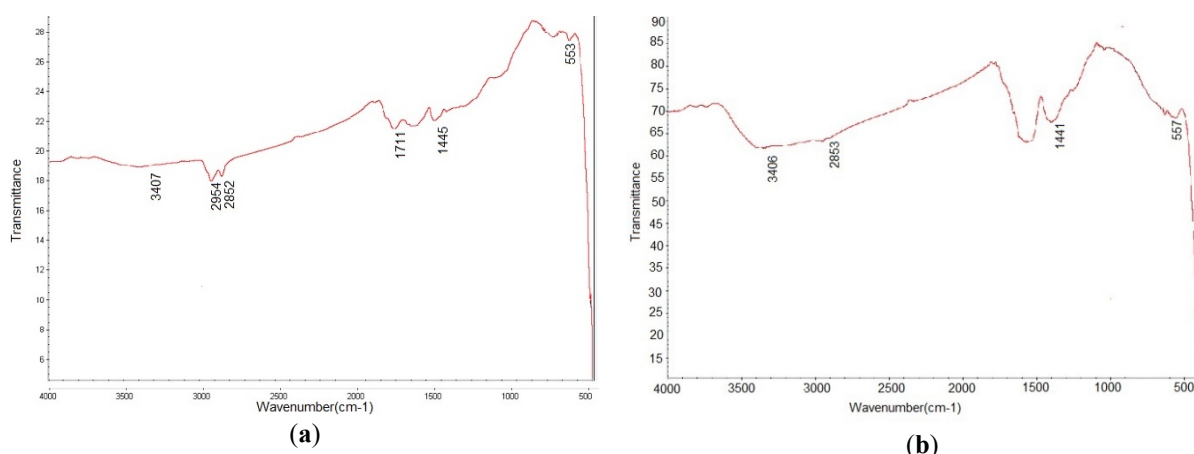


**Fig. 3.** FTIR result of synthesis by (a) mechanical and (b) magnetic mixtures [33].

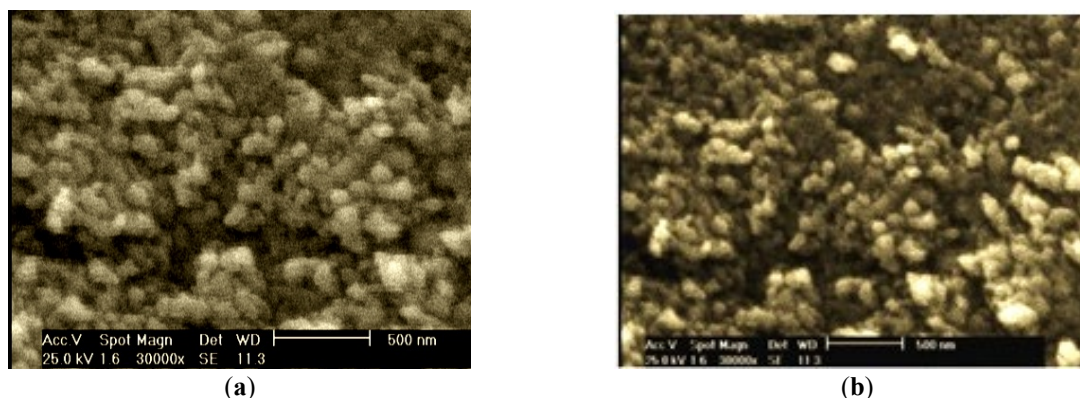


**Fig. 4.** SEM graph of  $\text{Fe}_3\text{O}_4$  nanoparticles synthesis by (a) mechanical and (b) magnetic stirrings [33].

#### 4. Conclusions

$\text{Fe}_3\text{O}_4$  nanoparticles were produced by the chemical precipitation method. Two samples were prepared separately, using mechanical and magnet stirring. The SEM images showed the morphology of the generated nanoparticles was near spherical and the average crystallite size of the magnetite nanoparticles was estimated via XRD analysis. The mean sizes were found to be 11 nm for the mechanically stirred sample and 13 nm for the magnetically stirred sample. Those sizes are suitable for technological applications. The XRD analysis showed that the generated magnetite nanoparticles have an inverse spinel crystallite structure. The VSM demonstrated the superparamagnetic behavior at room temperature. Therefore, magnetite nanoparticles are regarded as a soft magnetic material due to their low coercivity. FTIR absorption spectroscopy confirms the reverse spinel structure and the presence of the organic surfactant, elements in the samples. Measurements showed that nanoparticles are nearly spherical.

**Author Contributions:** conceptualization, H. R. Dehghanpour; methodology, H. R. Dehghanpour and P. Parvin; software, M. Gilaki; validation, H. R. Dehghanpour, M. Gilaki.; formal analysis, A. Younesi.; investigation, M. Gilaki.; resources, H. R. Dehghanpour; data curation, P. Parvin; writing—original draft preparation, H.R. Dehghanpour, M. Gilaki; writing—review and editing, H. R. Dehghanpour, P. Parvin; visualization, A. Younesi; supervision, H. R. Dehghanpour.

**Funding:** This research did not receive external funding.

**Conflicts of Interest:** The authors declare no conflict of interest.

#### References

- Raj, K.; Moskowitz, B.; Casciari, R. Advances in ferrofluid technology. *Journal of Magnetism and Magnetic Materials* **1995**, *149*, 174–180.
- Leslie-Pelecky, D. L.; Rieke, R. D. Magnetic properties of nanostructured materials. *Chemistry of Materials* **1996**, *8*(8), 1770.
- Majetich, S. A.; Scott, J. H.; Kirkpatrick, E. M.; Chowdary, K.; Gallagher, K.; McHenry, M. E. Magnetic nanoparticles and magnetocrystalline anisotropy. *Nanostructured Materials* . **1997**, *9*( 1–8), 291.
- Kodama, R. H. Magnetic nanoparticles. *Journal of Magnetism and Magnetic Materials* **1999**, *200* ( 1–3), 359.
- Sugimoto, M. The past, present, and future of ferrites. *Journal of the American Ceramic Society* **1999**, *82*( 2), 269.
- Turtelli, R. S.; Duong, G. V.; Nunes, W.; Grössinger, R.; Knobel, M. Magnetic properties of nanocrystalline  $\text{CoFe}_2\text{O}_4$  synthesized by modified citrate-gel method. *Journal of Magnetism and Magnetic Materials* **2008**, *320*, e339–e342.
- Murdock, E. S.; Simmons, R. F.; Davidson, R. Roadmap for 10 Gbit/in<sup>2</sup> media: Challenges. *IEEE Transactions on Magnetics* **1992**, *28*(5), 3078–3083.
- Niu, D.; Li, Y.; Ma, Z.; Diao, H.; Gu, J.; Chen, H.; Zhao, W.; Ruan, M.; Zhang, Y.; Shi, J. Preparation of uniform, water-soluble, and multifunctional nanocomposites with tunable sizes. *Advanced Functional Materials* **2010**, *20*( 5), 773.
- Pradeep, A.; Priyadharsini, P.; Chandrasekaran, G. Sol–gel route of synthesis of nanoparticles of  $\text{MgFe}_2\text{O}_4$  and XRD, FTIR and VSM study. *Journal of Magnetism and Magnetic Materials* **2008**, *320*( 21), 2774.
- García-Cerda, L. A.; Torres-García, V. A.; Matutes-Aquino, J. A.; Ayala-Valenzuela, O. E. Magnetic nanocomposites: Preparation and characterization of Co-ferrite nanoparticles in a silica matrix. *Journal of Alloys and Compounds* **2004**, *369*, 148.
- Wu, J. H.; Ko, S. P.; Liu, H. L.; Jung, M. H.; Lee, J. H.; Ju, J. S.; Kim, Y. K. Sub 5 nm  $\text{Fe}_3\text{O}_4$  nanocrystals via coprecipitation method. *Colloids and Surfaces A* **2008**, *313–314*, 268.
- Doh, S. G.; Kim, E. B.; Lee, B. H.; Oh, J. H. Characteristics and synthesis of Cu–Ni ferrite nanopowders by coprecipitation method with ultrasound irradiation *Journal of Magnetism and Magnetic Materials* **2004**, *272–276*, 2238.

13. Ji, G. B.; Tang, S. L.; Ren, S. K.; Zhang, F. M.; Gu, B. X.; Du, Y. W. Simplified synthesis of single-crystalline magnetic  $\text{CoFe}_2\text{O}_4$  nanorods by a surfactant-assisted hydrothermal process. *Journal of Crystal Growth* **2004**, 270, 156.
14. Zhang, W.-D.; Xiao, H. M.; Zhu, L. P.; Fu, S. Y. Templatefree solvothermal synthesis and magnetic properties of novel singlecrystalline magnetite nanoplates. *Journal of Alloys and Compounds* **2009**, 477, 736–738.
15. Baruwati, B.; Rana, R. K.; Manorama, S. V. Further insights in the conductivity behavior of nanocrystalline  $\text{NiFe}_2\text{O}_4$ . *Journal of Applied Physics* **2007**, 101(1), 014302.
16. Zhao L.; Zhang, H.; Xing, Y.; Song, S.; Yu, S.; Shi, W.; Guo, X.; Yang, J.; Lei, Y.; Cao, F. Studies on the magnetism of cobalt ferrite nanocrystals synthesized by hydrothermal method. *Journal of Solid State Chemistry* **2008**, 181(2), 245.
17. Yang, H.; Zhang, X.; Ao, W.; Qiu, G. Formation of  $\text{NiFe}_2\text{O}_4$  nanoparticles by mechanochemical reaction. *Materials Research Bulletin* **2004**, 39(6), 833.
18. Li, X. D.; Yang, W. S.; Li, F.; Evans, D. G.; Duan, X. Stoichiometric synthesis of pure  $\text{NiFe}_2\text{O}_4$  spinel from layered double hydroxide precursors for use as the anode material in lithium-ion batteries. *Journal of Physics and Chemistry of Solids* **2006**, 67, 1286.
19. Dehghanpour, H. R. Physical and chemical properties of  $\text{NiFe}_2\text{O}_4$  nanoparticles prepared by combustion and ultrasonic bath methods. *Russian Journal of Applied Chemistry* **2016**, 89(1), 80.
20. Dehghanpour, H. R.; Delshad, L. Mn ferrite nanoparticle generation in distilled water using Nd:yttrium aluminum garnet laser. *Journal of Laser Applications* **2014**, 26(2), 022008.
21. Dehghanpour, H. R. Generation of soft ferrite nanoparticles by pulsed laser ablation in liquids. *Journal of Russian Laser Research* **2013**, 34(5), 453.
22. Amara, D.; Felner, I.; Nowik, I.; Margel, S. Synthesis and characterization of Fe and  $\text{Fe}_2\text{O}_4$  nanoparticles by thermal decomposition of triiron dodecacarbonyl. *Colloids and Surfaces A* **2009**, 339, 106.
23. Lu, J.; Jiao, X.; Chen, D.; Li, W. Solvothermal Synthesis and Characterization of  $\text{Fe}_2\text{O}_4$  and  $\gamma\text{-Fe}_2\text{O}_3$  nanoplates. *Journal of Physical Chemistry C* **2009**, 113(10), 4012.
24. Zhou, H.; Yi, R.; Li, J.; Su, Y.; Liu, X. Microwave-assisted synthesis and characterization of hexagonal  $\text{Fe}_2\text{O}_4$  nanoplates. *Solid State Sciences* **2010**, 12(1), 99.
25. Hessien, M. M. Synthesis and characterization of lithium ferrite by oxalate precursor route. *Journal of Magnetism and Magnetic Materials* **2004**, 320(21), 2800.
26. Dehghanpour, H. R.  $\text{CoFe}_2\text{O}_4$  nanoparticles structural and magnetic stability relative to ball milling. *Russian Journal of Applied Chemistry* **2016**, 89, 846.
27. Dehghanpour, H. R. Nickel Ferrite Nanoparticle Generation by Combustion Method and the Nanoparticle Structural and Magnetic Characterization and the Effect of Ball Milling. *IEEE Transactions on Magnetics* **2016**, 53(1), 2300105.
28. Dehghanpour, H. R. High coercivity induced in nickel ferrite nanoparticles by mechanical milling. *Journal of Structural Chemistry* **2018**, 59(5), 1122–1127.
29. Wang, C.; Zhang, W. Synthesizing nanoscale iron particles for rapid and complete dechlorination of TCE and PCBs. *Environmental Science and Technology* **1997**, 31(7), 2154–2156.
30. Kooij, E. S.; Gălcă, A. C.; Poelsema, B. Field induced phase segregation in ferrofluids. *Journal of Colloid and Interface Science* **2008**, 327(1), 261–265.
31. Huang, C.; Zhang, H.; Sun, Z.; Zhao, Y.; Chen, S.; Tao, R.; Liu, Z. Porous  $\text{Fe}_3\text{O}_4$  nanoparticles: Synthesis and application in catalyzing epoxidation of styrene. *Journal of Colloid and Interface Science* **2011**, 364(2), 298–303.
32. Jeong, U.; Teng, X.; Wang, Y.; Yang, H.; Xia, Y. Superparamagnetic colloids Controlled synthesis and niche applications. *Advanced Materials* **2007**, 19(1) 33–60.
33. Dehghanpour, H. R. The Effects of Surfactant Changing on Physical Properties of  $\text{Fe}_3\text{O}_4$  Nanoparticles Produced in Coprecipitation Method. *Russian Journal of Inorganic Chemistry* **2020**, 65(8), 1282–1286.
34. Dehghanpour, H. R. pH, molar ratio of ferrous to ferric ions and surfactant presence effects on physical properties of iron oxide nanoparticles generated by co-precipitation method. *Journal of Coordination Chemistry* **2020**, 73(24), 3452–3464.

**Publisher's Note:** IIKII stays neutral with regard to jurisdictional claims in published maps and institutional affiliations.

**Copyright:** © 2022 The Author(s). Published with license by IIKII, Singapore. This is an Open Access article distributed under the terms of the [Creative Commons Attribution License](https://creativecommons.org/licenses/by/4.0/) (CC BY), which permits unrestricted use, distribution, and reproduction in any medium, provided the original author and source are credited.